ELECTROMAGNETIC SCATTERING BY SIMPLE ICE CRYSTAL SHAPES

Richard Silveira

August 25, 2006

Abstract

We consider the problem of electromagnetic scattering by simple ice crystal shapes. This has important meteorological applications, where understanding the behaviour of scattered radiation through clouds can enable the remote measurement of quantities such as ice crystal sizes and cloud optical depths. We solve Maxwell's equations to set up a boundary-value transmission problem. The Helmholtz equation is satisfied inside and outside the ice crystal with complex and real wavenumbers respectively. We apply Green's Representation Theorem to reformulate the problem as a set of boundary integral equations, for which the unknowns are the total field and its normal derivative. We solve via a Galerkin boundary element method, originally developed for acoustic scattering, and investigate its effectiveness. Some encouraging results are obtained, though we note the limitations of applying such a method to our problem. Further work is suggested that may alleviate these constraints.

Acknowledgements

I would like to thank my supervisors for this project, Professor Simon Chandler-Wilde and Dr. Stephen Langdon, for their generous time and support, and everyone on the Msc course and in the Maths department who has made this year tremendously enjoyable. I would also like to acknowledge the NERC for funding this work.

Declaration

I confirm this report is all my own work and any material taken from other sources has been fully and properly acknowleged.

Richard Silveira

List of Figures

List of Tables

1 Introduction

Electromagnetic scattering is an important application in many areas of science and industry, from the

2 The Boundary-Value Transmission Problem

2.1 From Maxwell's equations to the Helmholtz equation

We start with Maxwell's equations, which describe the propagation of electromagnetic waves in a medium.

$$
\begin{aligned}
\cdot E &= \frac{\rho}{} \\
\cdot H &= 0 \\
\times E + \mu\frac{\partial H}{\partial t} &= 0 \\
\times H - \frac{\partial E}{\partial t} - \sigma E &= 0
\end{aligned}
$$

where σ is thelumedium.

that $E(x)$ and $H(x$

We denote the domain of the scatterer in the plane of incidence by D, with the exterior domain $R^2 \setminus \bar{D}$. The total field outside is given by $u^t(\mathrm{x}) = u^i(\mathrm{x}) + u^s(\mathrm{x})$, where $u^s(\mathrm{x})$ is the scattered field. Inside the total field is equal to the transmitted field, $u_0(\mathrm{x})$. Outside we take the parameter values as those for a vacuum, which is a good approximation for air. Therefore we have $\sigma = 0, \quad = {}_0$ (electric permittivity of free space) and $\mu = \mu_0$ (magnetic permeability of free space). Inside, we take $\mu = \mu_0$, since ice is non-magnetic, with σ and   taking the appropriate values for ice (we will continue to denote by σ and μ for clarity). Thus we have the scattered and transmitted fields satisfying the Helmholtz equation in both domains.

$$\Delta u^s(\mathrm{x}) + k^2 u^s(\mathrm{x}) = 0, \quad k^2 = \omega^2 \mu_0 \ {}_0 \tag{2.1}$$

$$\Delta u_0(\mathrm{x}) + k_0^2 u_0(\mathrm{x}) = 0, \quad k_0^2 = \omega^2 \mu_0 \ + i\mu_0 \sigma \omega \tag{2.2}$$

The significance of the complex wavenumber is that the transmitted field decays inside D, due to the non-zero conductivity. In the limit $\sigma \to \infty$

$$
\begin{aligned}
-u_0(\mathrm{x}) &= \int_\Gamma \left(u_0(\mathrm{y}) \frac{\partial \Phi(k_0, \mathrm{x}, \mathrm{y})}{\partial \mathrm{n}(\mathrm{y})} - \frac{\partial u_0(\mathrm{y})}{\partial \mathrm{n}} \Phi(k_0, \mathrm{x}, \mathrm{y}) \right) ds(\mathrm{y}) \\
&= \int_\Gamma \left(u^t(\mathrm{y}) \frac{\partial \Phi_0(\mathrm{x}, \mathrm{y})}{\partial \mathrm{n}(\mathrm{y})} - \frac{\partial u^t(\mathrm{y})}{\partial \mathrm{n}} \Phi(k_0, \mathrm{x}, \mathrm{y}) \right) ds(\mathrm{y}), \quad \mathrm{x} \in D \qquad (2.3) \\
u^s(\mathrm{x}) &= \int_\Gamma \left(u^s(\mathrm{y}) \frac{\partial \Phi(k, \mathrm{x}, \mathrm{y})}{\partial \mathrm{n}(\mathrm{y})} - \frac{\partial u^s(\mathrm{y})}{\partial \mathrm{n}} \Phi(k, \mathrm{x}, \mathrm{y}) \right) ds(\mathrm{y}), \quad \mathrm{x} \in R^2 \setminus \bar{D} \qquad (2.4)
\end{aligned}
$$

In (2.3) we have used the boundary condition that $u^t = u_0$ on Γ. $\Phi(k, \mathrm{x}, \mathrm{y})$ and $\Phi(k_0, \mathrm{x}, \mathrm{y})$ are the fundamental solutions to the 2-D Helmholtz equations (2.1) and (2.2)

$$
\begin{aligned}
\Phi(k, \mathrm{x}, \mathrm{y}) &:= \frac{i}{4} H_0^{(1)}(k|\mathrm{x} - \mathrm{y}|) \\
\Phi(k_0, \mathrm{x}, \mathrm{y}) &:= \frac{i}{4} H_0^{(1)}(k_0|\mathrm{x} - \mathrm{y}|)
\end{aligned}
$$

$H_0^{(1)}(z)$ is the Hankel function of the first kind of order zero. An important feature to note that is that as $z \to 0$, $H_0^{(1)}(z) \to -\infty\, i$ and is undefined at the origin. This is relevant to some of the integrals we encounter later. We choose to solve for the total field outside, u^t, rather than the scattered field u^s. The reason for this is that if we solve for the scattered field we are left with a singular integral, whereas if we consider the total field, we obtain two such terms whose singularities are equal and opposite and cancel each other out (see (4.7)). We therefore add the following term to both sides of (2.4),

$$
u^i(\mathrm{x}) = \int_\Gamma \left(u^i(\mathrm{y}) \frac{\partial \Phi(k, \mathrm{x}, \mathrm{y})}{\partial \mathrm{n}(\mathrm{y})} - \frac{\partial u^i}{\partial \mathrm{n}}(\mathrm{y}) \Phi(k, \mathrm{x}, \mathrm{y}) \right) ds(\mathrm{y}) + u^i(\mathrm{x}), \quad \mathrm{x} \in R^2 \setminus \bar{D}
$$

We then have

$$
u^t(\mathrm{x}) = \int_\Gamma \left(u^t(\mathrm{y}) \frac{\partial \Phi(k, \mathrm{x}, \mathrm{y})}{\partial \mathrm{n}(\mathrm{y})} - \frac{\partial u^t(\mathrm{y})}{\partial \mathrm{n}} \Phi(k, \mathrm{x}, \mathrm{y}) \right) ds(\mathrm{y}) + u^i
$$

$$
\begin{aligned}
S\psi(x) &:= \int_\Gamma \psi(y)\Phi(k, x, y)\,ds(y) \\
S_0\psi(x) &:= \int_\Gamma \psi(y)\Phi(k_0, x, y)\,ds(y) \\
K\psi(x) &:= \int_\Gamma \psi(y)\frac{\partial \Phi(k, x, y)}{\partial n(y)}\,ds(y) \\
K_0\psi(x) &:= \int_\Gamma \psi(y)\frac{\partial \Phi(k_0, x, y)}{\partial n(y)}\,ds(y) \\
K\ \psi(x) &:= \int_\Gamma \psi(y)\frac{\partial \Phi(k, x, y)}{\partial n(x)}\,ds(y) \\
K_0\psi(x) &:= \int_\Gamma \psi(y)\frac{\partial \Phi(k_0, x, y)}{\partial n(x)}\,ds(y) \\
T\psi(x) &:= \frac{\partial}{\partial n(x)}\int_\Gamma \psi(y)\frac{\partial \Phi(k, x, y)}{\partial n(y)}\,ds(y) \\
T_0\psi(x) &:= \frac{\partial}{\partial n(x)}\int_\Gamma \psi(y)\frac{\partial \Phi(k_0, x, y)}{\partial n(y)}\,ds(y)
\end{aligned}
$$

We take (2.8)-(2.6) and (2.9)-(2.7) to give us the following integral equations

$$
(2 + K_0 - K)u^t + (S - S_0)\frac{\partial u^t}{\partial n} = 2u^i \tag{2.10}
$$

$(2 + K$

the main difference being that we seek here to approximate two unknowns. We also note the integral equations we would obtain if we solved for the scattered field, u^s.

052016[()55()]21126433054[()]1001214242660c[]0004360021130542110012142426422202

$$(2 + K_0 - K)u^t + (S - S_0)\frac{\partial u^t}{\partial n} \quad = \quad -u^i - K_0 u^i + S_0 \frac{\partial u^i}{\partial n}$$

$$(2 + K - K_0)\frac{\partial u^t}{\partial n} + (T_0 - T)u^t \quad T_0 u^i + K$$

7.97Tf6.2454.505Td[(i)]TJF1510.909Tf5.806-4.5058s10.909Tf

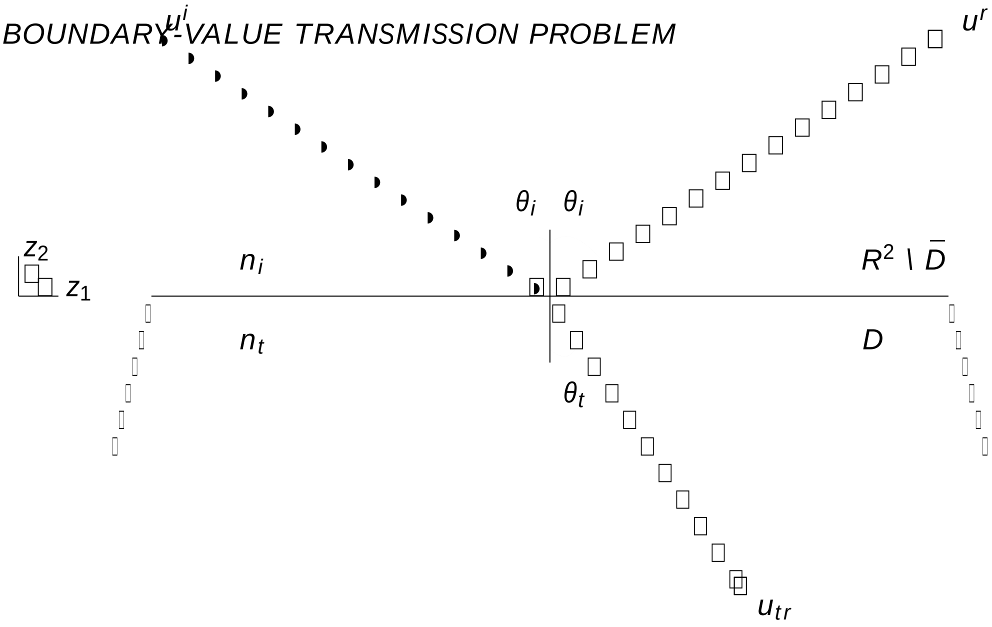
u^i
u^r
θ_i θ_i
z_2
z_1
n_i
$R^2 \setminus \bar{D}$
n_t
D
θ_t
u_{tr}

$$R = n\cos(\theta_i) - n_t\cos(\theta_t)$$

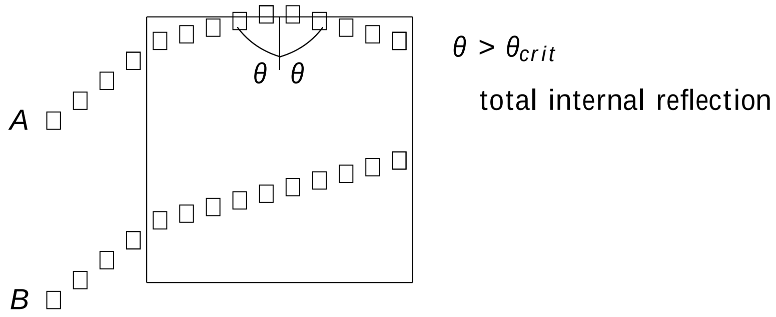

Figure 2.3: Multiple ray contributions at a shadow side

from one side to another that follow a straight line path through D (marked B in figure 2.3) and waves that undergo total internal reflection one or more times before arriving at the given side (marked A in figure 2.3).

We do not attempt here the difficult task of obtaining an analytical expression for the leading order behaviour on a shadow side. Instead, we use the same approximation as [6], that $u^t \approx 0$ and $\frac{\partial u^t}{\partial n} \approx 0$. We remind ourselves that we are only solving for u^t on Γ, hence we need no approximation for u_0.

2.6 Modified integral equations

Having identified the leading order behaviour, we separate it off and formulate the integral equations. We let

$$
\begin{aligned}
u^t &= \phi_u + \Psi_u \\
\frac{\partial u^t}{\partial n} &= \phi_{\partial u/\partial n} + \Psi_{\partial u/\partial n}
\end{aligned}
$$

where

$$\Psi_u = \begin{cases} (1+R)u^i & \text{illuminated sides} \\ 0 & \text{shadow sides} \end{cases}$$

$$\Psi_{\partial u/\partial n} = \begin{cases} (1-R)\frac{\partial u^i}{\partial n} & \text{illuminated sides} \\ 0 & \text{shadow sides} \end{cases}$$

Then (2.10) and (2.11) become

$$(2I + K_0 - K)\phi_u + (S - S_0)\phi_{\partial u/\partial n} = (2u^i - \Psi_u) - (K_0 - K)\Phi_u - (S - S_0)\Phi_{\partial u/\partial n} \qquad (2.17)$$

$$(T_0 - T)\phi_u + (2I + K' - K_0')\phi_{\partial u/\partial n} = (2\frac{\partial u}{\partial n} - \Psi_{\partial u/\partial n}) - (T_0 - T)\Phi_u - (K' - K_0')\Phi_{\partial u/\partial n} \qquad (2.18)$$

Thus our new unknowns are ϕ_u and $\phi_{\partial u/\partial n}$. What do these represent? We can make a comparison with the acoustic scattering problem in [6] to gain a better understanding. As we do here, the leading order behaviour (incident plus reflected field) is subtracted, and (2.12) becomes

$$(I + i\eta S + K')\phi = 2i\eta u^i + 2\frac{\partial u^i}{\partial n} - (I + i\eta S + K')\Psi$$

where $1/k\partial u^s/\partial n = \phi + \Psi$. $\Psi = 2\partial u^i/\partial n$ on illuminated sides, and zero on shadow sides. ϕ represents the field that is diffracted round the corners of the polygon. We note that $\Psi = \Psi_{\partial u/\partial n}$ when $R = -1$. This corresponds to the case when $k_0 >> k$, or when $\sigma \to \infty$, and as we have said, the electric field in D tends to zero in this case. Then we have the same exterior scattering problem since u^t must be zero on Γ if it is zero inside, due to the boundary condition that the electric field is continuous across the boundary. So for large values of σ, ϕ_u and $\phi_{\partial u/\partial n}$ represent the diffracted field on the boundary. If σ is small or zero, then we expect that the incident wave will be primarily transmitted through D. Then u^t and $\partial u^t/\partial n$ are not negligible on shadow sides (see figure 2.5.2). Then ϕ_u and $\phi_{\partial u/\partial n}$ will continue to represent the diffracted field on illuminated sides, while on shadow sides they will represent the diffracted and transmitted fields.

3 Parameterisation and the Approximation Space

3.1 Parameterisation

To solve the boundary integral equations, we need to discretise the boundary, and parameterise the variables x and y on the boundary. Schematically we have

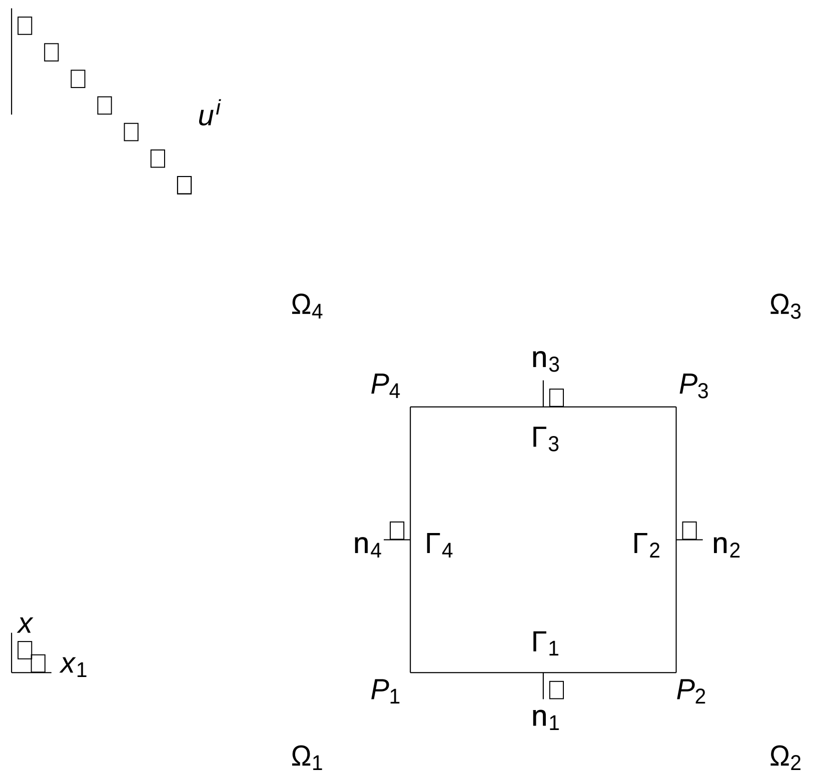

θ is measured anti-clockwise from the downwards vertical, and $d = (\sin\theta, -\cos\theta)$ is the direction of propagation. The unit normal on Γ_l is given by $\mathbf{n} = (n_1, n_2) = (b_l, -a_l)$, with

$$\frac{\partial u^i}{\partial \mathbf{n}(\mathbf{x})} = \nabla_{\mathbf{x}} u^i \cdot \mathbf{n}(\mathbf{x}) = \frac{\partial u^i}{\partial x_1} n_1 + \frac{\partial u^i}{\partial x_2} n_2 = (b_l \sin\theta + a_l \cos\theta) u^i$$

We let s and t be parametric representations for $\mathbf{x}$ and $\mathbf{y}$ respectively, with $s \in \Gamma_l$ and $t \in \Gamma_j$. Then s and t are the distance traversed anti-clockwise around the boundary, with $s = t = 0$ at P_1. On Γ_l we have

$$\begin{aligned} \mathbf{x}(s) &= P_l + s\left(\frac{P_{l+1} - P_l}{L_l}\right), \quad s \in (0, L_l) \\ &= P_l + \left(s - \sum_{k=1}^{l-1} L_k\right)\left(\frac{P_{l+1} - P_l}{L_l}\right), \quad s \in \Gamma_l \end{aligned}$$

Thus

$$\begin{aligned} x_1(s) &= p_l + \left(s - \sum_{k=1}^{l-1} L_k\right)\left(\frac{p_{l+1} - p_l}{L_l}\right), \quad s \in \Gamma_l \\ x_2(s) &= q_l + \left(s - \sum_{k=1}^{l-1} L_k\right)\left(\frac{q_{l+1} - q_l}{L_l}\right), \quad s \in \Gamma_l \end{aligned}$$

Now we define

$$
\begin{aligned}
a_l &:= \frac{p_{l+1} - p_l}{L_l} \\
b_l &:= \frac{q_{l+1} - q_l}{L_l} \\
c_l &:= p_j - a_l \sum_{k=1}^{l-1} L_k \\
d_l &:= q_j - b_l \sum_{k=1}^{l-1} L_k
\end{aligned}
$$

which gives us the parameterised variables $x(s)$ and $y(t)$

$$x$$

$v_j^{\pm}$ on the sides of the polygon. Essentially, the $v_j^{\pm}$ are peaked near the corners (increasingly peaked for more acute corners) and approximately constant away from the corners. This is illustrated in figure 3.2. The peak at A is due to $v_j^+ e^{iks}$, while the peak at B is due to $v_{j+1}^- e^{-iks}$, so that the diffracted wave causes peaked behaviour on the side it is diffracted onto. We do not expect a significant contribution to the peak at B from $v_j^+ e^{iks}$, nor do we expect $v_{j+1}^- e^{-iks}$ to affect the peak at A.

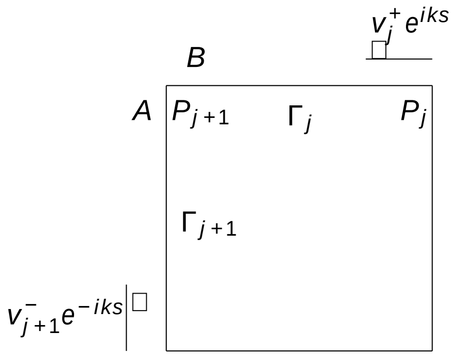

Figure 3.2: Diffracted behaviour at a corner

Thus on Γ_j, v_j^+ will be peaked near P_j, and approximately constant away from P_j and towards P_{j+1}. v_j^- will exhibit the opposite, being peaked near P_{j+1}, and approximately constant as we move towards P_j. The novelty of the Galerkin scheme in [6] is that the $v_j^{\pm}$ are approximated by piecewise polynomials instead of 1191.741]TJ/F34 10.90.909 Tf 768(the)8(e)]

3.2.1 The mesh and basis functions

We define the mesh identically to that in [6]. On each side we have two meshes to fit the behaviour of $v_j^{\pm}$. We term $gridx$ and $gridy$ be the meshes around the boundary consisting of the individual v_j^+ and v_j^- respectively, so that $gridx = [v_1^+, \cdots, v_{n_v}^+]$ and $gridy = [v_1^-, \cdots, v_{n_v}^-]$. We let n_{gx} and n_{gy} be the number of elements in $gridx$ and $gridy$. We denote these by Γ_j^+ and Γ_j^-. On Γ_j^+ the grading is high (ie the nodes are very close together) at P_j (where v_j^+

The basis functions, $\rho_j(t)$ are defined by

$$\rho_j(t) := \frac{e^{ik\sigma_j t} \; \xi_{[y_j, y_{j+1}]}}{(y_{j+1} - y_j)}$$

where $\xi_{[y_j, y_{j+1}]}$ is the characteristic function for the interval $[y_j, y_{j+1}]$. $\xi_{[y_j, y_{j+1}]} = 1$ if $s \quad [y_j, y_{j+1}]$, zero otherwise.

There are a few points to note here. ν is the degree of polynomial we use in our basis function. Here we use piecewise constants so $\nu = 0$. On $\Gamma_j^{\pm}$ we have a composite mesh. The high grading occurs on the interval $[0, \lambda]$ with N mesh points separated by a polynomial grading. On the interval $[\lambda, A]$ there is a geometric grading for $\hat{N}_{A,\lambda,q}$ mesh points. The choice of N ensures that the polynomial and geometric meshes exhibit a smooth transition. We take $A = L_j$ so that the mesh covers every side in both directions. We also note that the mesh grading is determined by α_j, which in turn is determined by the corner angle ω_j. The dependence is such that the approximation error in ϕ in [6] is equidistributed across the intervals of the mesh.

Lastly we note that for the basis function $\rho_j, \sigma_j = +1$ if ρ_j is on $gridx$ and -1 if it is on $gridy$.

4 The Galerkin Method

We recall the integral equations (2.17) and (2.18)

$$(2I + K_0 - K)\phi_u + (S - S_0)\phi_{\partial u/\partial n} = (2u^i - \Psi_u) - (K_0 - K)\Phi_u - (S - S_0)\Phi_{\partial u/\partial n}$$

$(T_0 -$ [illegible]

$$\phi_u = \sum_{j=1}^{n_g} u_j \rho_j(s), 0 \leq s \leq L$$

$$
\begin{bmatrix}
A_{11} & A_{12} & \cdots & B_{11} & B_{12} & \cdots \\
A_{21} & \ddots & \ddots & B_{21} & \ddots & \ddots \\
\vdots & \ddots & \ddots & \vdots & \ddots & \ddots \\
C_{11} & C_{12} & \cdots & D_{11} & D_{12} & \cdots \\
C_{21} & \ddots & \ddots & D_{21} & \ddots & \ddots \\
\vdots & \ddots & \ddots & \vdots & \ddots & \ddots
\end{bmatrix}
\begin{bmatrix}
u_1 \\ u_2 \\ \vdots \\ v_1 \\ v_2 \\ \vdots
\end{bmatrix}
=
\begin{bmatrix}
(F, \rho_1) \\ (F, \rho_2) \\ \vdots \\ (G, \rho_1) \\ (G, \rho_2) \\ \vdots
\end{bmatrix}
$$

In the following sections we describe the evaluation of the integrals in the matrix and right hand vector. Once we have these, we solve the matrix equation (using the inbuilt solve function in Matlab) to find the co-efficients u_i and v_i, which completes our approximation to ϕ_u and $\phi_{\partial u/\partial n}$ via (4.1) and (4.2). Then we compute the field everywhere using (2.3) and (2.5), but substituting $u^t = \phi_u + \Psi_u$ and $\partial u^t/\partial n = \phi_{\partial u/\partial n} + \Psi_{\partial u/\partial n}$. Then

$$
\begin{aligned}
-u_0(\mathrm{x}) &= \int_\Gamma \left\{ (\phi_u + \Psi_u)\frac{\partial \Phi_0(\mathrm{x},\mathrm{y})}{\partial \mathrm{n}(\mathrm{y})} - (\phi_{\partial u/\partial n} + \Psi_{\partial u/\partial n})\Phi(k_0, \mathrm{x}, \mathrm{y}) \right\} ds(\mathrm{y}), \quad \mathrm{x} \in D \\
u^t(\mathrm{x}) &= \int_\Gamma \left\{ (\phi_u + \Psi_u)\frac{\partial \Phi(k,\mathrm{x},\mathrm{y})}{\partial \mathrm{n}(\mathrm{y})} - (\phi_{\partial u/\partial n} + \Psi_{\partial u/\partial n})\Phi(k, \mathrm{x}, \mathrm{y}) \right\} ds(\mathrm{y}) + u^i(\mathrm{x}), \quad \mathrm{x} \in R^2 \setminus \bar{D}
\end{aligned}
$$

4.1 Left Hand Side

We have five integrals to determine for the left hand side of the matrix equation.

$$
\begin{aligned}
L_1 &= (2\rho_j, \rho_m) \\
L_2 &= ((K_0 - K)\rho_j, \rho_m) \\
L_3 &= ((K' - K_0')\rho_j, \rho_m) \\
L_4 &= ((S - S_0)\rho_j, \rho_m) \\
L_5 &= ((T_0 - T)\rho_j, \rho_m)
\end{aligned}
$$

4.1.1 L_1

$$\begin{aligned}(2\rho_j, \rho_m) &= 2\int_0^L \rho_j(s)\bar{\rho}_m(s)ds \\ &= 2\int_{supp(\rho_j)\cap supp(\rho_m)} \frac{e^{iks(\sigma_j-\sigma_m)}}{\sqrt{(y_{m+1}-y_m)}\sqrt{(y_{j+1}-y_j)}}\end{aligned} \tag{4.3}$$

The basis functions are defined only on their intervals, so L_1 is non-zero where the basis functions overlap. Denoting rh and lh to be the ends of the overlap,

$$L_1 = \begin{cases} \dfrac{2\left(e^{ik(\sigma_j-\sigma_m)rh} - e^{ik(\sigma_j-\sigma_m)lh}\right)}{ik(\sigma_j-\sigma_m)\sqrt{(y_{j+1}-y_j)(y_{m+1}-y_m)}} & \sigma_j = \sigma_m \\ \dfrac{2(rh-lh)}{\sqrt{(y_{j+1}-y_j)(y_{m+1}-y_m)}} & \sigma_j = \sigma_m \end{cases}$$

4.1.2 L_2 and L_3

We recall that

$$K\psi(\mathrm{x}) = 2\int_\Gamma \frac{\partial\Phi(k,\mathrm{x},\mathrm{y})}{\partial \mathrm{n}(\mathrm{y})}\psi(\mathrm{y})ds(\mathrm{y})$$

where

$$\frac{\partial\Phi(k,\mathrm{x},\mathrm{y})}{\partial \mathrm{n}(\mathrm{y})} = \nabla_{\mathbf{y}}\Phi(k,\mathrm{x},\mathrm{y})\cdot \mathrm{n}(\mathrm{y}) = \frac{\partial\Phi(k,\mathrm{x},\mathrm{y})}{\partial y_1}n_1 + \frac{\partial\Phi(k,\mathrm{x},\mathrm{y})}{\partial y_2}n_2$$

$$\Phi(k,\mathrm{x},\mathrm{y}) = \frac{i}{4}H_0^{(1)}(kR), R = |\mathrm{x}-\mathrm{y}| = \left[(x_1-y_1)^2 + (x_2-y_2)^2\right]^{\frac{1}{2}}$$

We have that $\frac{d}{dz}H_n^{(1)}(z) =$ yjxosmqdmmmdzzdH $^{(1)}$

$$K'\psi(\mathrm{x}) = 2\int_\Gamma \frac{-ik}{4}\frac{H_1^{(1)}(kR)}{R}\,[(x_1 - y_1)n_1(\mathrm{x}) + (x_2 - y_2)n_2(\mathrm{x})]\,\psi(\mathrm{y})ds(\mathrm{y})$$

Now we parameterise using s and t, $s \in \Gamma_l$ and $t \in \Gamma_j$ (see section 3.1), to obtain the integrals in parameterised form

$$\begin{aligned} K\psi(s) &= 2\int_\Gamma k(s,t)\psi(t)dt \\ K'\psi(s) &= 2\int_\Gamma k'(s,t)\psi(t)dt \end{aligned}$$

where

$$\begin{aligned} k(s,t) &= \frac{ik}{4}\frac{H_1^{(1)}(kR)}{R}\,[(a_l b_j - b_l a_j)s + (c_l - c_j)b_j - (d_l - d_j)a_j] \\ k'(s,t) &= \frac{-ik}{4}\frac{H_1^{(1)}(kR)}{R}\,[(a_l b_j - b_l a_j)t + (c_l - c_j)b_l - (d_l - d_j)a_l] \end{aligned}$$

Then

$$\begin{aligned} (k_0 - k)(s,t) &= \frac{i}{4}\frac{(k_0 H_1^{(1)}(k_0 R) - kH_1^{(1)}(kR))}{R}\,[(a_l b_j - b_l a_j)s + (c_l - c_j)b_j - (d_l - d_j)a_j] \\ (k' - k_0')(s,t) &= \frac{-i}{4}\frac{(kH_1^{(1)}(kR) - k_0 H_1^{(1)}(k_0 R))}{R}\,[(a_l b_j - b_l a_j)t + (c_l - c_j)b_l - (d_l - d_j)a \end{aligned}$$

and

$$L_3 = 2\int_{y_m}^{y_{m+1}}\int_{y_j}^{y_{j+1}} \frac{(k - k_0)(s,t)e^{ik(\sigma_j t-\sigma_m s)}}{(y_{m+1} - y_m)(y_{j+1} - y_j)} dtds$$

We evaluate these, and all the integrals that follow that are not analytic, numerically using Gaussian quadrature. Further details are given in section 4. We observe that for $l = j$, when s and t lie on the same side of the polygon $(k_0 - k)(s,t) = (k - k_0)(s,t) = 0$, and therefore L_2 and L_3 are zero.

4.1.3 L_4

$S\psi(\mathrm{x}) = 2\int_\Gamma \Phi(k,\mathrm{x},\mathrm{y})\psi(\mathrm{y})ds(\mathrm{y})$, and analogous to the evaluation of L_3 and L_4, we have the parameterised kernel $(s - s_0)(s,t) = \frac{i}{4}(H_0^{(1)}(kR) - H_0^{(1)}(k_0R))$. For $l = j$,

$$L_4 = 2\int_{y_m}^{y_{m+1}}\int_{y_j}^{y_{j+1}} \frac{(s - s_0)(s,t)e^{ik(\sigma_j t-\sigma_m s)}}{(y_{m+1} - y_m)(y_{j+1} - y_j)} dtds$$

For $l = j$, we can evaluate some of the integral analytically. We note that $R = |s - t|$, and use the following integral representation for the Hankel function [9, 12.31]

$$H_0^{(1)}(s) = \frac{-2i}{}$$

$$I(r) = \int_{y_m}^{y_{m+1}} \int_{y_j}^{y_{j+1}} e^{(i-r)k|s-t|+ik(\sigma_j t-\sigma_m s)} \; s) \; s) \; s$$

□

$$\frac{\partial}{\partial x_1}\frac{\partial \Phi(k,\mathrm{x},\mathrm{y})}{\partial \mathrm{n}(\mathrm{y})} = \frac{\partial}{\partial x_1}\left(\frac{ik}{4}H_1^{(1)}(kR).R^{-1}.\left[(x_1-y_1)n_1(\mathrm{y})+(x_2-y_2)n_2(\mathrm{y})\right]\right)$$

$$= \frac{i}{4}\left(\begin{array}{llll} \left(\frac{H_1^{(1)}(kR)}{kR}-H_1^{(2)}(kR)\right) & \frac{k^2(x_1-y_1)}{R} & \frac{1}{R} & \left[(x_1-y_1)n_1(\mathrm{y})+(x_2-y_2)n_2(\mathrm{y})\right] \\ +kH_1^{(1)}(kR) & & \frac{-(x_1-y_1)}{R^3} & \left[(x_1-y_1)n_1(\mathrm{y})+(x_2-y_2)n_2(\mathrm{y})\right] \\ +kH_1^{(1)}(kR) & & \frac{-(x_1-y_1)}{R^3} & n_1(\mathrm{y}) \end{array}\right)$$

$$
\begin{aligned}
H_1^{(1)}(z) &= J_1(z) + iY_1(z) \\
&\approx \frac{z}{2\Gamma(2)} - \frac{2i\Gamma(1)}{\pi z}, \quad \text{as } z \to 0 \\
&= \frac{z}{2} - \frac{2i}{\pi z}
\end{aligned}
$$

Therefore the kernel becomes

$$(t_0 - t)(s, t) \quad = \quad (b^2$$

4.2.1 R_1 and R_2

$$(2u^i - 2\Psi_u, \rho_m) = \int_{y_m}^{y_{m+1}} \frac{(2u^i - 2\Psi_u)e^{-ik\sigma_m s}}{\sqrt{(y_{m+1} - y_m)}} ds$$

On shadow sides, $\Psi_u = 0$, so we have

$$R_1 = \int_{y_m}^{y_{m+1}} \frac{2e^{ik[(a_l s + c_l)sin\theta - (b_l s + d_l)cos\theta] - ik\sigma_m s}}{\sqrt{(y_{m+1} - y_m)}} ds \tag{4.8}$$

On illuminated sides, $\Psi_u = (1 + R)u^i$, $(2u^i - 2\Psi_u) = -2Ru^i$, so we have (4.8) mulitplied by a factor of $-R$. We also have $\Psi_{\partial u/\partial n} = 0$ on shadow sides, so

$$R_2 = \int_{y_m}^{y_{m+1}} \frac{2\left[b_l \sin\theta + a_l \cos\theta\right] e^{ik[(a_l s + c_l)sin\theta - (b_l s + d_l)cos\theta] - ik\sigma_m s}}{\sqrt{(y_{m+1} - y_m)}} ds \tag{4.9}$$

On illuminated sides, $\Psi_u = (1 - R)\partial u^i/\partial n$, $(2\partial u^i/\partial n - 2\Psi_{\partial u/\partial n}) = 2R\partial u^i/\partial n$, and we have (4.9) multiplied by R. Thus

$$R_1 = \begin{cases} \frac{2e^{ik(c_l sin\theta - d_l cos\theta)}}{ik(a_l sin\theta - b_l cos\theta - \sigma_m)\sqrt{(y_{m+1} - y_m)}} \left(e^{ik(a_l sin\theta - b_l cos\theta - \sigma_m)y_{m+1}} - e^{ik(a_l sin\theta - b_l cos\theta - \sigma_m)y_m} \right) & \text{shadow side} \\ \frac{-2R_l e^{ik(c_l sin\theta - d_l cos\theta)}}{ik(a_l sin\theta - b_l cos\theta - \sigma_m)\sqrt{(y_{m+1} - y_m)}} \left(e^{ik(a_l sin\theta - b_l cos\theta - \sigma_m)y_{m+1}} - e^{ik(a_l sin\theta - b_l cos\theta - \sigma_m)y_m} \right) & \text{illuminated side} \end{cases}$$

Likewise

$$R_2 = \begin{cases} \frac{2(b_l sin\theta + a_l cos\theta)e^{ik(c_l sin\theta - d_l cos\theta)}}{ik(a_l sin\theta - b_l cos\theta - \sigma_m)\sqrt{(y_{m+1} - y_m)}} \left(e^{ik(a_l sin\theta - b_l cos\theta - \sigma_m)y_{m+1}} - e^{ik(a_l sin\theta - b_l cos\theta - \sigma_m)y_m} \right) & \text{shadow side} \\ \frac{2R_l(b_l sin\theta + a_l cos\theta)e^{ik(c_l sin\theta - d_l cos\theta)}}{ik(a_l sin\theta - b_l cos\theta - \sigma_m)\sqrt{(y_{m+1} - y_m)}} \left(e^{ik(a_l sin\theta - b_l cos\theta - \sigma_m)y_{m+1}} - e^{ik(a_l sin\theta - b_l cos\theta - \sigma_m)y_m} \right) & \text{illuminated side} \end{cases}$$

4.2.2 R_3, R_4, R_5, R_6

$$\begin{aligned} R_3 &= ((K_0 - K)\Psi_u, \rho_m) \\ &= 2\int_{y_m}^{y_{m+1}} \int_{\sum_{j=1}^{n_s} L_j}^{L} \frac{(k_0 - k)(s, t)\Psi(t)dt e^{-ik\sigma_m s}}{\sqrt{(y_{m+1} - y_m)}} ds \end{aligned}$$

We change the order of integration and split the integral over the illuminated sides to a sum of the integrals over each illuminated side, denoting the reflection co-efficient on Γ_k by R_k

$$
\begin{aligned}
R_3 &= 2 \sum_{j=n_s+1}^{n} \int_{\sum_{p=1}^{j-1} L_p}^{\sum_{p=1}^{j} L_p} \left(\int_{y_m}^{y_{m+1}} \frac{(k_0 - k)(s,t)\Psi(t) ds e^{-ik\sigma_m s}}{\sqrt{(y_{m+1} - y_m)}} \right) \Psi(t) dt \\
&= 2 \sum_{j=n_s+1}^{n} (1 + R_k) e^{ik(c_j sin\theta - d_j cos\theta)} \int_{\sum_{p=1}^{j-1} L_p}^{\sum_{p=1}^{j} L_p} \int_{y_m}^{y_{m+1}} \frac{(k_0 - k)(s,t) e^{ik[(a_j sin\theta - b_j cos\theta)t - \sigma_m s]}}{\sqrt{(y_{m+1} - y_m)}} dsdt
\end{aligned}
$$

Similarly

$$
\begin{aligned}
R_4 &= 2 \sum_{j=n_s+1}^{n} (1 - R_k)\,[b_j \cos\theta + a_j \sin\theta]\, e^{ik(c_j sin\theta - d_j cos\theta)} \int_{\sum_{p=1}^{j-1} L_p}^{\sum_{p=1}^{j} L_p} \int_{y_m}^{y_{m+1}} \frac{(k - k_0)(s,t) e^{ik[(a_j sin\theta - b_j cos\theta)t - \sigma_m s]}}{\sqrt{(y_{m+1} - y_m)}} dsd \\
R_5 &= 2 \sum_{j=n_s+1}^{n} (1 - R_k)\,[b_j \cos\theta + a_j \sin\theta]\, e^{ik(c}
\end{aligned}
$$

$$
\begin{aligned}
J(r) \;=\; & \left(\frac{e^{((i-r)k-ik\sigma_m)x_{m+1}} - e^{((i-r)k-ik\sigma_m)x_m}}{(i-r)k-ik\sigma_m}\right)\left(\frac{e^{((r-i)k+ik\sigma_j)x_m} - e^{((r-i)k+ik\sigma_j)y_j}}{(r-i)k+ik\sigma_j}\right)\\
- & \left(\frac{e^{((i-r)k_0-ik\sigma_m)x_{m+1}} - e^{((i-r)k_0-ik\sigma_m)x_m}}{(i-r)k_0-ik\sigma_m}\right)\left(\frac{e^{((r-i)k_0+ik\sigma_j)x_m} - e^{((r-i)k_0+ik\sigma_j)y_j}}{(r-i)k_0+ik\sigma_j}\right)\\
+ & \left(\frac{e^{((r-i)k-ik\sigma_m)x_{m+1}} - e^{((r-i)k-ik\sigma_m)x_m}}{(r-i)k-ik\sigma_m}\right)\left(\frac{e^{((i-r)k+ik\sigma_j)y_{j+1}} - e^{((i-r)k+ik\sigma_j)x_{m+1}}}{(i-r)k+ik\sigma_j}\right)\\
- & \left(\frac{e^{((r-i)k_0-ik\sigma_m)x_{m+1}} - e^{((r-i)k_0-ik\sigma_m)x_m}}{(r-i)k_0-ik\sigma_m}\right)\left(\frac{e^{((i-r)k_0+ik\sigma_j)y_{j+1}} - e^{((i-r)k_0+ik\sigma_j)x_{m+1}}}{(i-r)k_0+ik\sigma_j}\right)\\
+ & \frac{1}{(r-i)k-ik\sigma_m}\left(\frac{e^{(ik(\sigma_j-\sigma_m))x_{m+1}} - e^{(ik(\sigma_j-\sigma_m))x_m}}{ik(\sigma_j-\sigma_m)} - \frac{e^{(r-i)k(x_m-x_{m+1})+ik(\sigma_j x_{m+1}-\sigma_m x_m)} - e^{ik(\sigma_j-\sigma_m)x_m}}{(i-r)k+ik\sigma_j}\right)\\
- & \frac{1}{(r-i)k_0-ik\sigma_m}\left(\frac{e^{(ik(\sigma_j-\sigma_m))x_{m+1}} - e^{(ik(\sigma_j-\sigma_m))x_m}}{ik(\sigma_j-\sigma_m)} - \frac{e^{(r-i)k_0(x_m-x_{m+1})+ik(\sigma_j x_{m+1}-\sigma_m x_m)} - e^{ik(\sigma_j-\sigma_m)x_m}}{(i-r)k_0+ik\sigma_j}\right)\\
- & \frac{1}{(i-r)k-ik\sigma_m}\left(\frac{e^{(ik(\sigma_j-\sigma_m))x_{m+1}} - e^{(ik(\sigma_j-\sigma_m))x_m}}{ik(\sigma_j-\sigma_m)} - \frac{e^{ik(\sigma_j-\sigma_m)x_{m+1}} - e^{(r-i)k(x_m-x_{m+1})+ik(\sigma_j x_m-\sigma_m x_{m+1})}}{(r-i)k+ik\sigma_j}\right)\\
+ & \frac{1}{(i-r)k_0-ik\sigma_m}\left(\frac{e^{(ik(\sigma_j-\sigma_m))x_{m+1}} - e^{(ik(\sigma_j-\sigma_m))x_m}}{ik(\sigma_j-\sigma_m)} - \frac{e^{ik(\sigma_j-\sigma_m)x_{m+1}} - e^{(r-i)k_0(x_m-x_{m+1})+ik(\sigma_j x_m-\sigma_m x_{m+1})}}{(r-i)k_0+ik\sigma_j}\right)
\end{aligned}
$$

4.3 Gaussian quadrature

We have encountered many integrals that we cannot evaluate analytically, so we use Gaussian quadrature. Gaussian quadrature is a method of numerically approximating a definite integral by taking the weighted sum of the function value at a set of given nodes. ie

$$\int_{-1}^{1} g(y)dx \approx \sum_{i=1}^{n_q} w_i g(y_i)$$

where we have n_q nodes at the points y_i with corresponding weights w_i. For n_q quadrature points, the method yields an exact result for polynomials of degree $2n-1$. The integrals we encounter cover some interval $[a, b]$, so we transform the weights and nodes to an integral over $[-1, 1]$, which is the standard interval for Gaussian quadrature

$$
\begin{aligned}
w_i &\rightarrow w_i \times \frac{b-a}{2} \\
y_i &\rightarrow a + (b-a)\frac{(y_i+1)}{2}
\end{aligned}
$$

We have encountered two types of integral that we must approximate numerically, and we will briefly discuss how we apply the method of Gaussian quadrature in each case.

4.3.1 1-D non-oscillatory integrals

These are integrals of the form (4.4) and (4.10). After substitution, we evaluate with 100 quadrature points. This should produce a close approximation due to the non-oscillatory nature of the integral.

4.3.2 2-D oscillatory integrals

Every integral that does not fall into the previous category, we classify as a 2-D oscillatory integral. To begin, there is the obvious complication that we have only looked at approximating 1-D integrals. We carry out a 2-D quadrature as follows. We have the double integral

$$I = \int_a^b \int_c^d g(s,t)\,dt\,ds$$

We first compute an approximation to the inner integral, $h(s) = \int_c^d g(s,t)dt$ for $s_i, i = 1, \cdots, n_t$

$$h_{approx} = \sum_{i=1}^{n_t} w_i^t g(s_i, t_i)$$

and then approximate the outer integral using h_{approx}

$$I_{approx} = \sum_{i=1}^{n_s} w_i^s h_{approx}(s_i)$$

where n_s and n_t are the number of quadrature points we use in the s and t directions. There are two points to note here. Firstly, we require nodes in both directions, so we expect the quadrature to be

0.15^{n_q} is the minimum of a or c. The graded 2-D mesh is illustrated below. Note that it is not to scale (the actual mesh is very highly graded towards (a, c)) in order to clarify the sub-division of the interval.

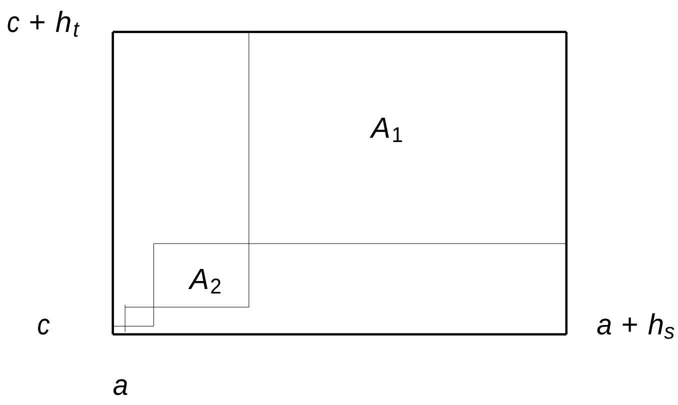

Figure 4.3: Graded mesh near a singularity or peak

The original integral is changed to individual integrals over $A_1, A_2, \cdots, A_{n_q+1}$. As n

to approximate $|\phi|$ well.

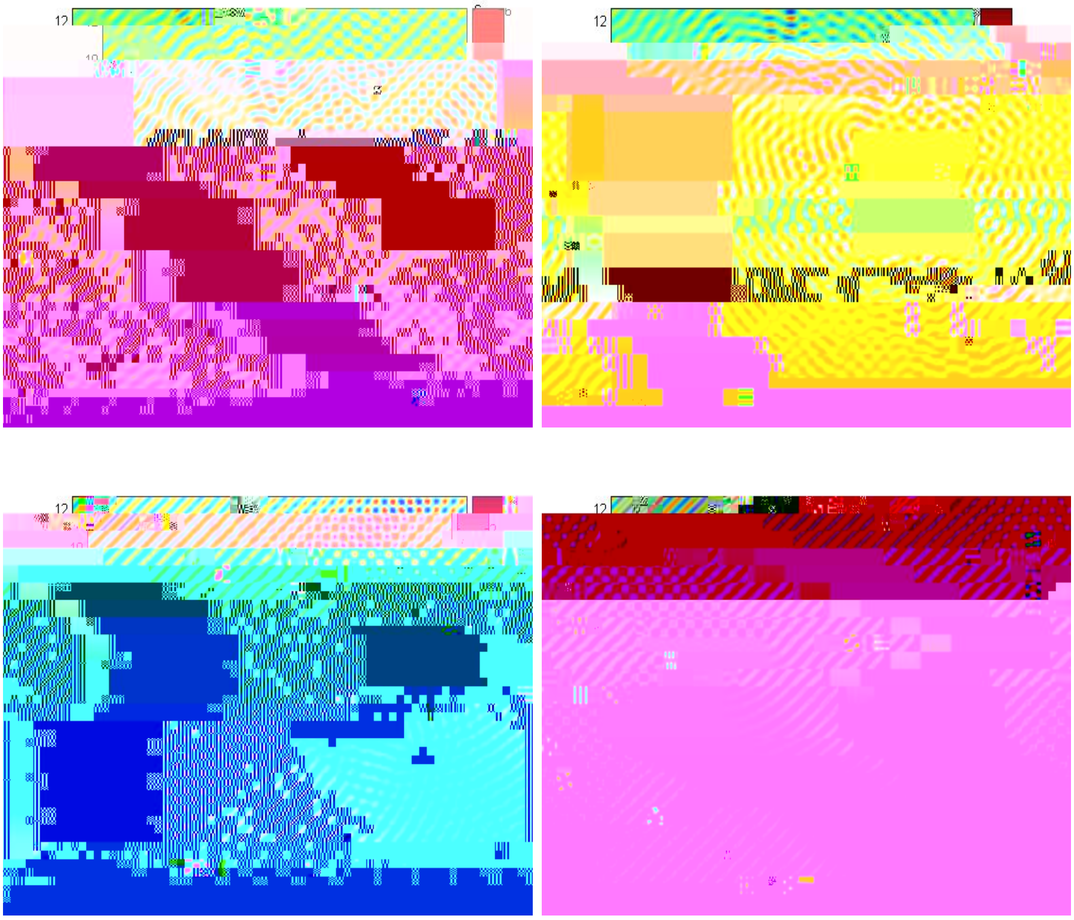

Figure 5.3: Acoustic scattering without subtraction of leading order behaviour, N=8,16,32,64

5.3 Transmission through a hexagonal ice crystal

We now consider transmission through a unit hexagonal ice crystal, side length 1. We use $n_{ice} = 1.31 + 0.01i$, with an incident wavenumber of 20 and angle of incidence $\theta = 49\pi/100$. We plot the total and transmitted fields for values of $N = 2, 4, 8, 16, 32$ and 64 (figures 5.5 and 5.6). The transmitted field is the total field minus the incident and reflected components, and is the part of the field that we approximate by ϕ_u and $\phi_{\partial u/\partial n}$. We also plot $|\phi_u|$ and $|\phi_{\partial u/\partial n}|$ on the boundary for $N = 32, 64$ and 128 (figure 5.7).

We obtain promising resulrTd[(and)]TJF3410.909Tf21.6460Td[

errors for $N = 2, 4, 8, 16, 32$ and 64 in table 5.2.

5.5 Transmission through a thin strip

Figure 5.10 shows plots of the total and transmitted field for an incident field ($k = 20, \theta = 49\pi/100$) on a rectangular strip with dimensions 1 by 10. Inside $k_0 = 34 + 5i$. We see very clear features; a partially reflected wave interacting with the incident wave; diffraction at either end of the strip giving rise to noticeable interference patterns in the shadow zone behind the obstacle; and a travelling wave inside the strip that is attenuated relatively strongly.

6 Conclusions and Further Work

We have adapted a Galerkin boundary element method for acoustic scattering and applied it to an electromagnetic transmission problem.

We have obtained encouraging results, but it is clear that this particular Galerkin boundary element solution of electromagnetic scattering problems can be enhanced using methods developed for acoustic scattering", with reference to the Galerkin scheme we have implemented. Despite a lack of tangible results, this method has showed decent promise and further work in this area should prove to be worthwhile.

References

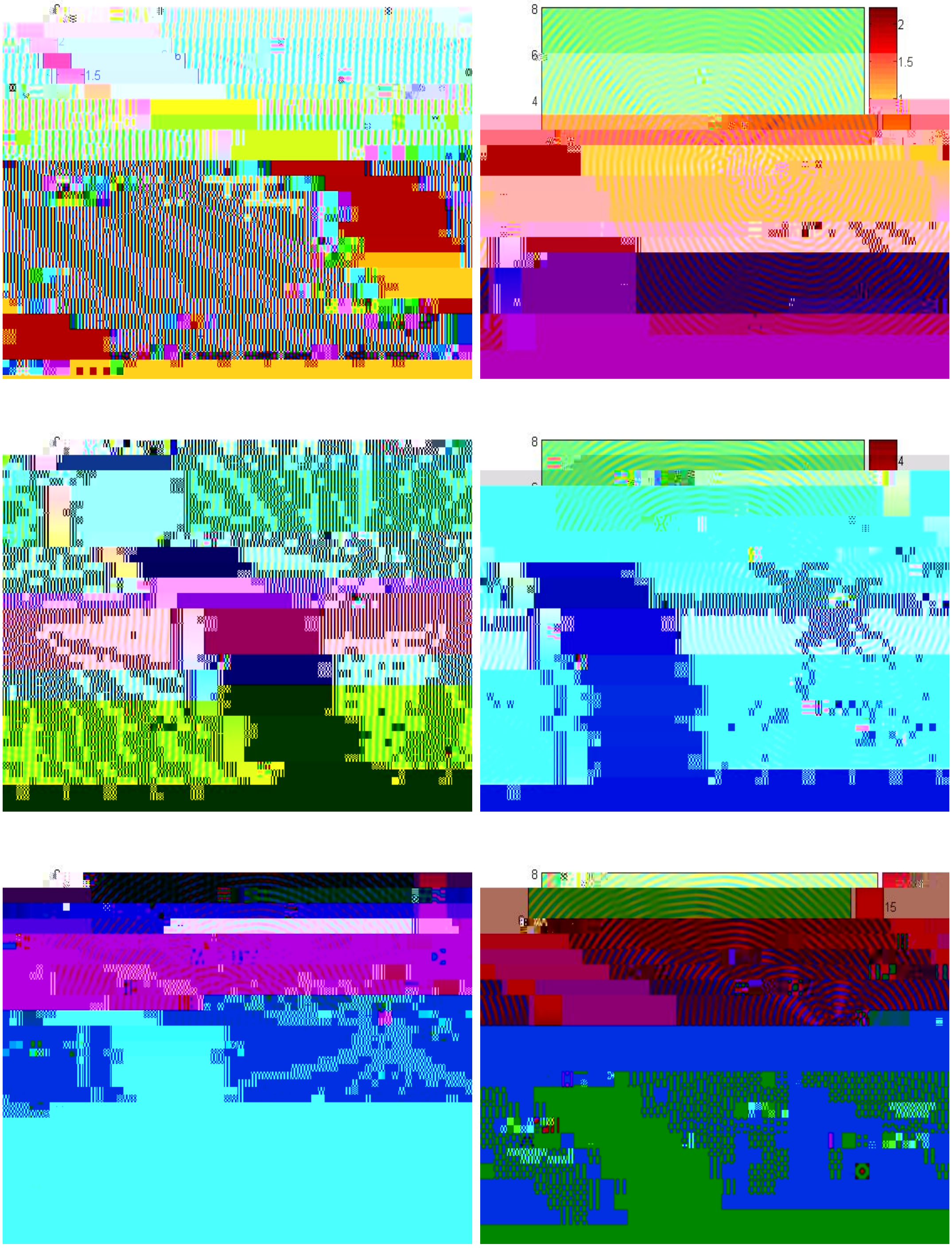

Figure 5.5: Total (left) and transmitted (right) fields for transmission through a hexagon, $k = 20, \theta = 49\pi/100, N = 2, 4, 8$

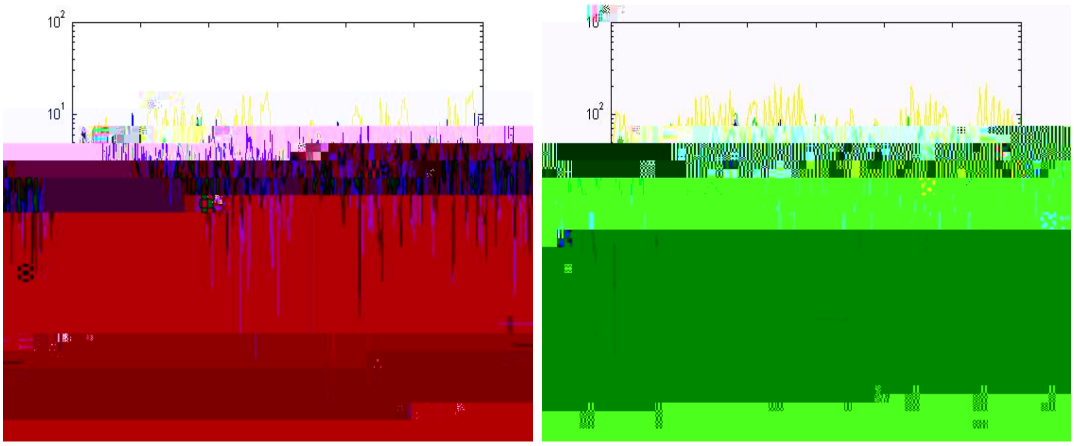

Figure 5.7: Plots of $|\phi_u|$ (left) and $|\phi_{\partial u/\partial n}|$ (right) on the boundary of the hexagon

N	Relative L^2 error ϕ_u	Relative L^2 error $\phi_{\partial u/\partial n}$
2	4.0397×10^{0}	3.5475×10^{0}
4	6.2566×10^{0}	5.5322×10^{0}
8	1.0164×10^{0}	1.3859×10^{0}
16	9.108×10^{-1}	1.6887×10^{0}
32	1.0020×10^{0}	8.262×10^{-1}
64	8.691×10^{-1}	3.284×10^{-1}

Table 5.2: Relative L2 errors for trianlge case

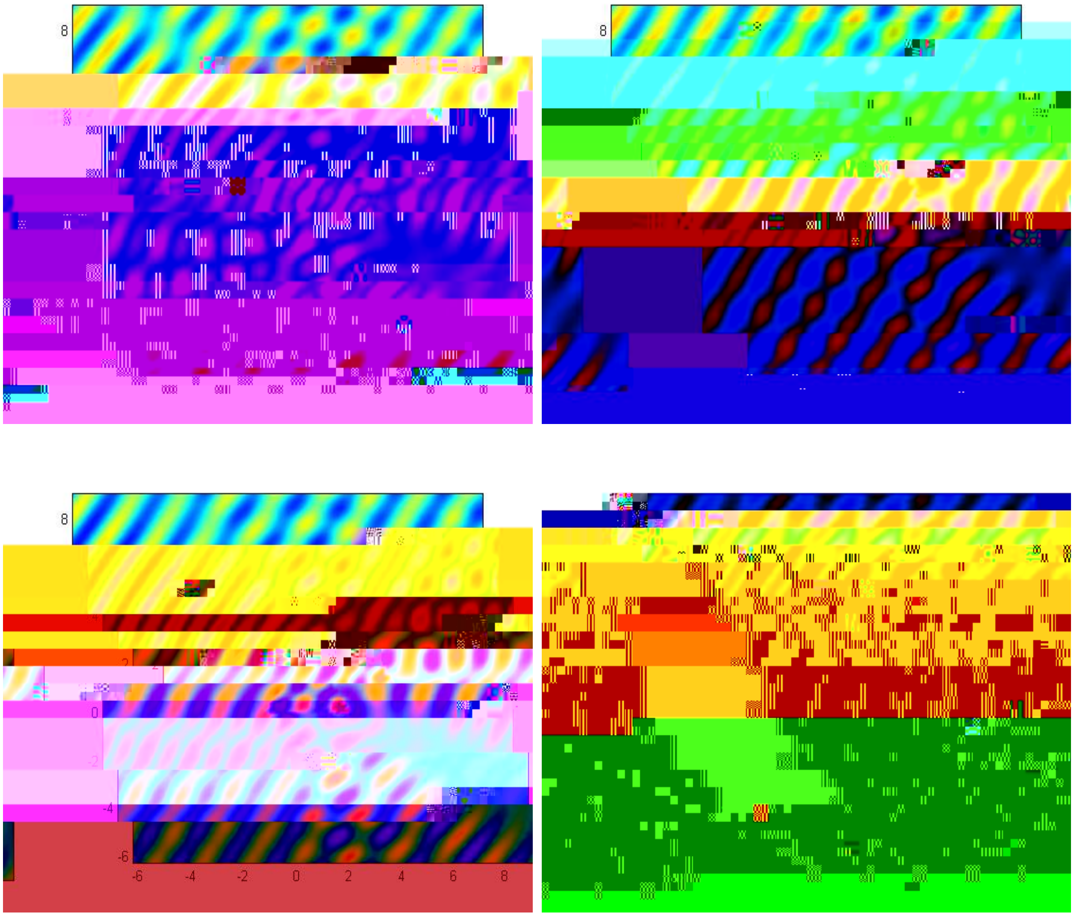

Figure 5.8: Total field plotted for transmission through a triangle, $k = 4, \theta = \pi/3, N = 16$ (top left), $N = 32$ (top right), $N = 64$ (bottom left) and $N = 128$ (bottom right)

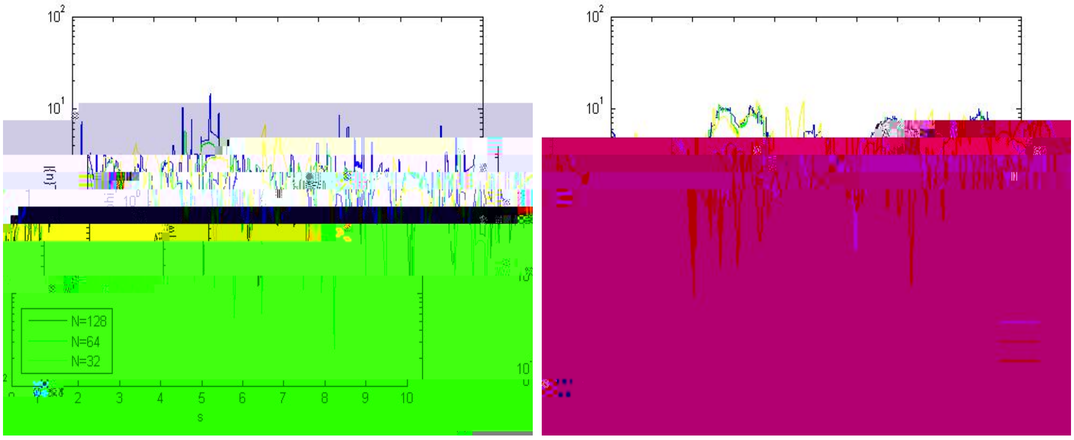

Figure 5.9: Plots of $|\phi_u|$ and $|\phi_{\partial u/\partial n}|$ on the boundary of the triangle

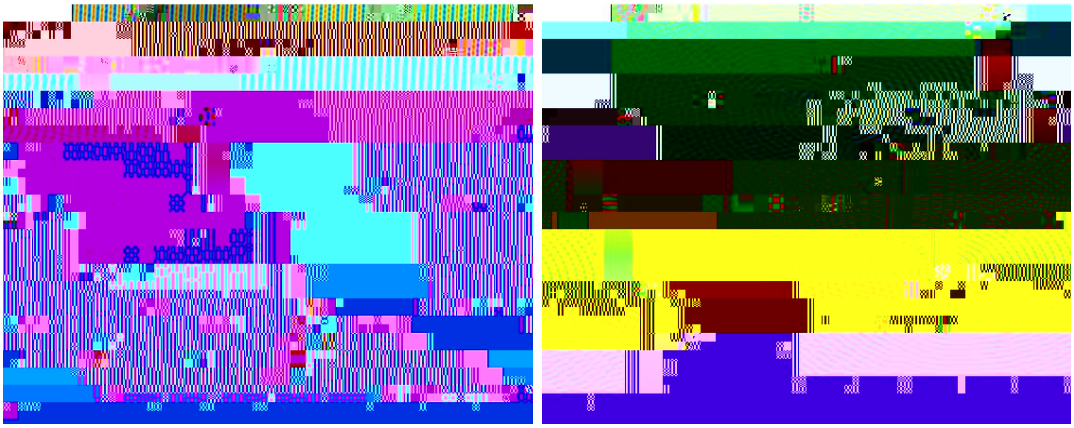

Figure 5.10: Total and transmitted fields for transmission through a thin strip